MATERIALS CHARACTERIZATION 84 (2013) 88–99

Available online at www.sciencedirect.com

ScienceDirect

www.elsevier.com/locate/matchar

Microstructures and properties of 2099 Al-Li alloy

*Yi Lin**, *Ziqiao Zheng*, *Shichen Li*, *Xiang Kong*, *Ye Han*

School of Materials Science and Engineering, Central South University, Changsha 410083, China

ARTICLE DATA

Article history:
Received 30 December 2012
Received in revised form 20 July 2013
Accepted 22 July 2013

Keywords:
2099 Al-Li alloy
Dynamic recrystallization
Texture
SCC

ABSTRACT

In this study, microstructures and properties of 2099 Al-Li alloy were investigated during the thermo-mechanical processing. Treated by two-step homogenization treatment (12 h at 510 °C + 36 h at 530 °C), the coarse dendritic structures cannot be observed in the alloy. At the same time, the level of grain boundary segregation was lowered, and a few of small AlCuFeMn/AlCuMn particles remained at the grain boundaries. Following homogenization treatment, the alloy was extruded at 470 °C. During extrusion process, dynamic recrystallization occurred in the surface layer of alloy, and the depth of dynamic recrystallized layer increased with solution treating at 540 °C. The central zone of alloy with solution treatment exhibited {111}<112> and {111}<110> textures, while {112}<110> texture presented at the surface zone. The corresponding central hardness of alloy in central zone was 95 HV, and the surface hardness was 120 HV. After solution treatment, two-step aging treatment was followed. In the peak-aged condition (12 h at 121 °C + 48 h at 152 °C), a large amount of T1 phases as well as δ′ phases precipitated in the matrix. The tensile strength, yield strength and elongation of alloy on peak aging were 613 MPa, 575 MPa, and 7.9%, respectively. The SCC susceptibility of alloy decreased with aging time, and the strength loss rate of alloy on over-aging was 5.5%.

1. Introduction

Al-Li series alloys are one of the age-hardenable aluminum alloys. Compared with the other aluminum alloys, higher elastic modulus, lower density, higher specific strength and more favorable damage tolerance properties can be attained in Al-Li alloys. Nowadays, the application of Al-Li alloys in the aerospace industry as structural components becomes an important way to reduce the weight, increase the payload and improve the fuel efficiency of aircraft [1].

At the end of 1990s, focus on Al-Li alloy containing greater than 2 wt.% Li was paid on, which possessed significantly reduced anisotropic properties compared to those currently available, and then a new Al-Li alloy C489 by optimization of chemical composition and processing technique was developed. Unfortunately, the elongation of C489 alloy in the peak-aged condition was too low to apply in aerospace industry. As a result of this research, C458, a derivative of the C489 alloy by lowering the Li content and increasing the Zr content, was developed. This C458 alloy possessed much higher elongation while also maintained similar isotropic mechanical properties. In 2003, C458 alloy was designed as 2099 by the Aluminum Association [2–4]. Nowadays, 2099-T83 extrusions have been qualified for A380 applications such as cross beams, seat rails, false rails, cockpit and emergency bay floor structures.

Some research works [2,5–9] on the 2099 alloy have been undertaken in the last 10 years. However, the evolution of microstructures and properties of the 2099 alloy during the whole thermo-mechanical processing, including homogenization treatment, extrusion, solution treatment and aging treatment, has not been reported. The final properties of alloy products depend on their microstructures, while the microstructures are influenced by thermo-mechanical processing.

* *Corresponding author at:* 932 South Road of Yue Lu Mountain, Changsha 410083, Hunan, China. Tel./fax: +86 731 88830270.
E-mail address: llinyi@163.com (Y. Lin).

1044-5803/$ – see front matter
http://dx.doi.org/10.1016/j.matchar.2013.07.015

Therefore, mastering the evolution laws of microstructures is beneficial to characterize the relation between microstructures and thermo-mechanical processing, to promote the improvement of processing technique and to optimize the properties of alloy. The present work was undertaken to investigate the evolution of microstructures and properties of the 2099 alloy during thermo-mechanical processing and discuss the mechanisms by which microstructures were formed in different conditions. These results can give indispensable information for optimizing the properties of the 2099 alloy.

2. Experimental

The 2099 alloy (Table 1) was prepared by liquid metallurgy route in an electrical resistance furnace. The permanent water-cooled cast-iron mould was used to shape the alloy in the form of Φ100 × 230 mm. The as-cast alloy was subjected to two-step homogenization treatment (12 h at 510 °C + 36 h at 530 °C) in the salt bath. After homogenization treatment, the alloy was extruded into a cylindrical rod of 16 mm diameter at 470 °C, and the extruded rod was machined into small tensile samples with lengths of 100 mm. These tensile samples were solution treated in a salt bath at 540 °C for 1 h followed by water quenching, and then stretched to 2.5% at room temperature. Finally, a two-step aging treatment (12 h at 121 °C + t at 152 °C, t-aging time) was followed.

Tensile tests were performed on MTS 858 testing machine in a displacement-controlled mode at a displacement rate of 2 mm/min. Cylindrical samples with gauge dimensions of 6 mm in diameter and 40 mm in length were used. Three samples per condition were tested. An extensometer attached to the sample gauge was used to determine strain and total elongation. The experimental errors in measurements of the stress and strain values were less than 2.5%.

The stress corrosion cracking (SCC) susceptibility of alloy in different aging conditions was studied using the slow strain rate test (SSRT). Cylindrical samples with gauge dimensions of 4 mm in diameter and 40 mm in length were adopted. The SSRTs, both in air and in 3.5% NaCl + 0.5% H_2O_2 aqueous solution, were performed at a constant strain rate of 2×10^{-6} s^{-1} in a universal testing machine.

Electrochemical experiments were carried out using three-electrode system. Saturated calomel was used as reference electrode. Platinum was regarded as auxiliary electrode, and alloy samples with different aging conditions were made as working electrode. The alloy samples had dimensions of 10 mm in diameter and 1 mm in thickness. The testing solution was 3.5% NaCl + 0.5% H_2O_2 aqueous solution. Before testing, samples were polished to mirror and degreased with ethanol.

Microstructural features were characterized by using optical microscope (OM, Lecia EC3), scanning electron microscope/electron back scattered diffraction (SEM/EBSD, Quanta 200) and transmission electron microscope (TEM, Tecnai G^2 200) analysis. Sample for EBSD was taken from solution-treated alloy along the extrusion direction as shown in Fig. 1. The samples were prepared by removing the top surface with SiC paper followed by electropolishing in a special electrolyte to obtain a good surface finish. Slices for TEM samples were cut from tensile samples and subsequently ground to less than 70 μm and punched into 3 mm discs. The thin foils were obtained by using electrothinning at 15 V. The electrolyte was a mixture of 75% methanol and 25% nitric acid, and thinning was performed at −25 °C.

Table 1 – Chemical composition of the 2099 alloy (wt.%).

Cu	Li	Mg	Zn	Mn	Ti	Zr	Be	Al
2.74	1.77	0.32	0.72	0.34	0.05	0.10	0.0001	Bal

3. Results and Discussion

3.1. Microstructures and Properties of Homogenized Alloy

3.1.1. As-cast Microstructure

Fig. 2(a) shows that the as-cast 2099 alloy characterized with coarse dendritic structure. SEM observation reveals that there were irregular net-shaped interdendritic phases with the size of up to 150 μm (Fig. 2(b)). The distribution of elements in the local region of as-cast alloy is shown in Fig. 3. It indicates that the distribution of alloying elements was inhomogeneous. The alloying elements of Cu and Fe were inclined to segregating at the grain boundaries. The energy-dispersive spectroscopy (EDS) results identified the main interdendritic phases were Al_2Cu containing trace elements, such as Zn, Mn or Fe.

The microsegregation to the grain boundaries is due to the non-equilibrium grain boundary segregation of solute elements [10]. The mechanism of non-equilibrium segregation relies on the formation of sufficient quantities of vacancy-solute atom complexes. When the melt is quickly cooled through a large temperature range, the equilibrium concentration of vacancies, and thus complexes, is reduced. This true equilibrium concentration cannot be realized during fast cooling conditions except at vacancy sinks. Such sinks are interfaces like grain boundaries and surfaces. Thus, vacancy concentration gradients are formed in quickly-cooled melt, and there is a net flow of vacancies towards the vacancy sinks. The vacancy-solute atom complexes are also carried down these gradients and solute atoms are thus deposited at the sink. This diffusion leads excess solute atoms to concentrate in the vicinity

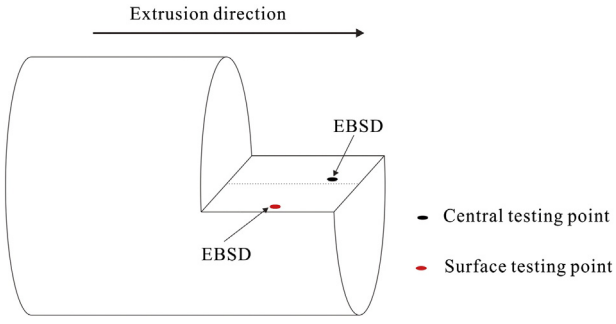

Fig. 1 – Schematic representation of the sample for EBSD analysis.